ChemComm

Accepted Manuscript

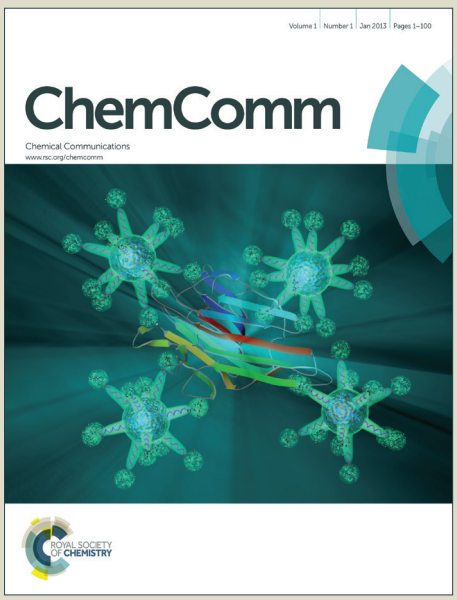

ROYAL SOCIETY OF CHEMISTRY

www.rsc.org/chemcomm

Low Energy Structural Dynamics and Constrained Libration of $Li(NH_3)_4$, the Lowest Melting Point Metal

A. G. Seel,[a,b], E. Zurek[c], A. J. Ramirez-Cuesta[d], K.R. Ryan[b] M. T. J. Lodge,[b] and P. P. Edwards*[b]

Received Xth XXXXXXXXXX 20XX, Accepted Xth XXXXXXXXX 20XX
First published on the web Xth XXXXXXXXXX 200X
DOI: 10.1039/b000000x

The lattice and molecular dynamics for the solid phases of currently the lowest melting-point metal, $Li(NH_3)_4$, are determined by incoherent inelastic neutron scattering. Measurements of internal molecular displacements and distortions of the $Li(NH_3)_4$ units have been modelled and assigned using Density Functional Theory calculations for the solid and molecular system. Inelastic neutron scattering measurement allow for the first determination of NH_3 librational transitions.

Few metal-insulator transitions (MITs) can be deemed as remarkable as that found in the system of Li-metal dissolved in anhydrous NH_3. The deep blue solutions of the dilute system undergo a phase change to the golden metallic liquid at 8 mole-percent metal (MPM) with the well documented phase separation occurring around 4 MPM, whereby the metallic phase floats above the semiconducting liquid phase. The electronic and structural properties for this system has been recently reviewed and revisited.[1,2]

The most concentrated system at 20 MPM, $Li(NH_3)_4$, forms a eutectic and is currently the metal with the lowest melting point known, solidifying only at 88.8 K.[3,4] Just as remarkable is the existence of a number of structural phase changes that occur in the solid system as it is cooled further. The highest temperature phase is cubic, conventionally termed Phase I, and persists in the short range $80 < T < 88.8$ K. This phase is not witnessed in $Li(ND_3)_4$,[5] and has been determined by quasielastic neutron scattering measurements to be a plastic phase.[6] Below 80 K the system crystallises into the orthorhombic Phase II, $I\bar{4}3d$, before finally crystallising in a further cubic phase with possible antiferromagnetic ordering, Phase III, $P2_13$. Tetrahedral geometry around Li is essentially retained in all phases, with only minor displacements of $Li(NH_3)_4$ units differentiating them. Studies on the vibrational dynamics of $Li(NH_3)_4$ are limited to molecular systems, including inelastic X-ray scattering[7] (IXS) in the liquid phase, theoretical studies[8] and determination of the vibrational structure of the excited electronic state in the gas phase[9].

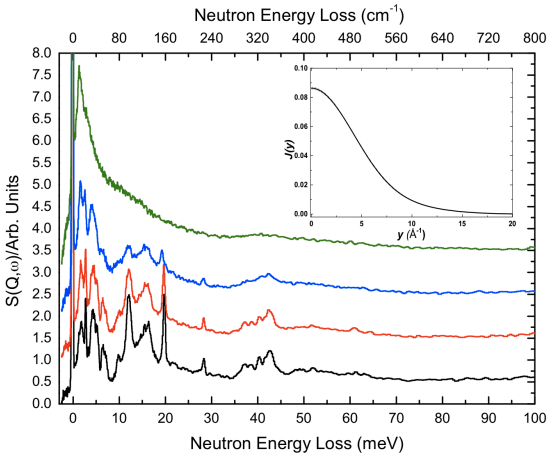

Fig. 1 Measured IINS spectra for solid $Li(NH_3)_4$ at various temperatures. 15 K (black), 25 K (red), 50 K (blue) and 85 K(green). Spectra have been offset along the y-axis for clarity. *Insert* Fitted neutron Compton profile at 4 K.

Incoherent inelastic neutron scattering (IINS) enables an examination of structural dynamics, in particular those of low energy, by the determination of the neutron dynamic structure factor, $S(\mathbf{q},\omega)$.[10,11] For an isotropic sample this can be written as

$$S(q,\omega_i) \propto \frac{(q\cdot u_i)^{2n}}{n!}\exp\left(-(q\cdot u_{Tot})^2\right). \qquad (1)$$

In the above expression q is the neutron wavevector transfer and ω_i is the frequency of the dynamical process i for fundamental transition $n = 1$. u_i is the root mean squared displacement for the atoms in the lattice mode and u_{Tot} is the root mean squared displacement for all atoms in all modes. $S(q,\omega)$ thus has a simple form, depending on a sum for each atom in the

[a] *ISIS Spallation Neutron Source, Rutherford Appleton Laboratory, Chilton, OX11 0QX, U.K.*
[b] *University of Oxford, Inorganic Chemistry Dept., South Parks Road, Oxford, OX13QR, U.K. Fax: 44 (0) 1865 272 656; Tel: 44 (0) 1865 272646; E-mail: peter.edwards@chem.ox.ac.uk*
[c] *Department of Chemistry, University at Buffalo, State University of New York, 331 NSC, Buffalo, NY 14260-3000, USA*
[d] *Chemical and Engineering Materials Division, Neutron Sciences Directorate, ORNL, 1 Bethel Valley Road, Oak Ridge, Tennessee 37831, USA*

system, weighted by its incoherent neutron scattering cross-section, σ^i, which for hydrogen far exceeds that for any other species (σ^i_H is 80.26 barn compared to σ^i_N and σ^i_{Li} values of 0.50 and 0.92 barn respectively).

Deep inelastic neutron scattering (DINS), also termed neutron Compton scattering, is the neutron analogue of Compton scattering of γ-photons from electrons in a system.[12] As such, DINS allows the determination of the nuclear momentum distribution *n(p)* for each atomic species of mass *M* in the system through the structure factor,

$$S(q,\omega) = \int n(p)\delta(\omega - \frac{\hbar q^2}{2M} - \frac{q\cdot p}{M})dp = \frac{q}{M}J_{IA}(q,y), \quad (2)$$

where J_{IA} is defined as the neutron Compton profile,[13,14]. The expression of the structure factor via the so called *y*-transform [$y = \frac{M}{q}(\omega - \frac{\hbar q^2}{2M})$] is convention in DINS, and is well documented for example in references [12] and [13].

Figure 1 shows the IINS spectra for $Li(NH_3)_4$ across its

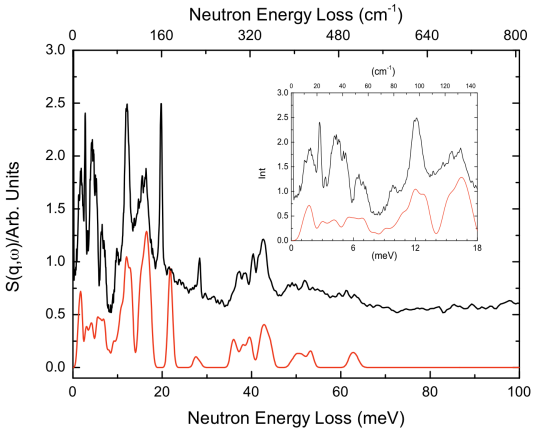

Fig. 2 Comparison between experimental (black) and calculated (red) IINS spectra. *inset*: low energy spectra. Experimental spectrum is for 15 K and calculated spectra are presented for the fundamental, 0-1, transition.

solid temperature phases. As can be seen there are a number of sharply defined features in the range of 1-50 meV (~8-400 cm^{-1}), with spectral intensity falling off sharply with increasing neutron energy loss. This rapid tailing off in intensity in the IINS spectra above 50 meV is indicative of a pronounced Debye-Waller factor (the exponential term in equation 1) in likelihood due to the molecular nature of the metal and low barrier to molecular displacement. This also accounts for the swift broadening and washing-out of features for temperatures above 25 K most noticeable in the plastic phase I at 85 K, despite these measurements still being at essentially cryogenic temperatures. The spectral features do not differ noticeably between solid phases. Also shown in figure 1 is the fitted $J(y)$ for the proton as determined from DINS measurement. No change was seen between solid phases, and from the second moment of $J(y)$ the average kinetic energy, $\langle E_K \rangle$, for the proton has been determined as 133.49 ± 3.70 meV.

Figure 2 compares IINS measurement at 20 K and DFT modelled spectra. The modelled spectra have been shifted -1.0 meV and demonstrate substantial agreement with experiment. This allows for an examination of the calculated eigenvectors and subsequent assignation of the IINS spectra.

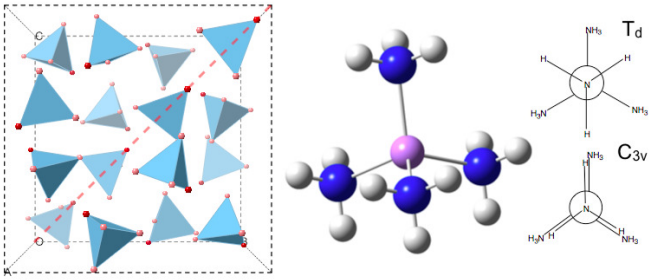

Fig. 3 *Left*: $Li(NH_3)_4$ solid ($I\bar{4}3d$) as viewed down the *a*-direction, demonstrating the two different N sites. $Li(NH_3)_4$ tetrahedra are blue, N1 red and N2 pink. The dashed line demonstrates the top-to-tail molecular alignment. *Middle*: The 'ideal' $Li(NH_3)_4$ molecule. *Right:* Comparison of T_d and C_{3v} molecular symmetry

A few considerations bear mentioning for the chemical interpretation of the IINS of this molecular metallic system. The stable geometry of the $Li(NH_3)_4$ in the gas phase has been calculated as an ideal tetrahedron of T_d symmetry[1]. It is interesting to note that this is not the case in the published crystal structures,[3] whereby NH_3 rotation reduces the symmetry to that of a C_{3v} molecule, with a slight increase of one Li-N bondlength. In the $I\bar{4}3d$ structure there are thus two nitrogen crystallographic sites, each $Li(NH_3)_4$ tetrahedron comprising one distorted N1 and three N2 atoms, whereby N1 is orientated towards the base of a neighbouring tetrahedral face comprising the 'undistorted' N2 atoms.[3] This is shown schematically in figure 3. The crystallographic data demonstrates that only slight shifts in these molecular units relative to this alignment occurs between phases.

As the features in the IINS spectra are indistinguishable between solid phases, we shall use, in as far as possible, a molecular language when discussing the vibrational dynamics in the solid. This is similar to the approach for the liquid found in reference [9].

Table 1 Internal modes of $Li(NH_3)_4$

IINS (meV)	DFT, T_d Molecule (meV)	DFT C_{3v} Molecule (meV)	IXS* (meV)	Description
2.7	2.9 (A_2)	-4.1	-	NH_3 libration
10.0	9.05 (E)	9.1	9.0	Li-N tetrahedral bend
-	4.06 (T_1)	9.10, 10.58	-	NH_3 libration
12.0	11.7 (T_2)	12.39, 12.71	18.0	Li-N tetrahedral bend
16.1	-	-	-	NH_3 (N2) librations with tetrahedral distortion
19.8	-	-	-	NH_3 (N1) libration
28.4	27.47 (A_1)	26.14	27.0	Symmetric Li-N stretch
37.1, 38.4	37.90 (T_2)	36.94, 37.53	40	NH_3 tilt with Li rattle
40.4, 42,5	38.50 (T_1)	39.71, 39.85	-	NH_3 tilt
-	47.77 (E)	48.44	-	NH_3 tilt
-	58.11 (T_2)	56.48, 56.54	-	NH_3 tilt with Li rattle

The T_d symmetry of the isolated $Li(NH_3)_4$ molecule gives rise to the 21 internal vibrational modes involving bends and distortions of the $Li(NH_3)_4$ units with no changes in N-H bondlengths, defined as $A_1 + A_2 + 2E + 2T_1 + 3T_2$. Descent to C_{3v} symmetry splits the T modes into an A and E mode.

As can be seen in figure 2, features are only witnessed in the IINS spectrum up to 45 meV ($\sim$360 cm^{-1}). These modes have been assigned and collected in table 1 with their measured and calculated values.

The IINS measurements are in agreement with available data from IXS, as well as DFT for both the solid and molecular systems in this study. The highest energy modes measured can be assigned to the tilting of NH_3 groups. These modes are split in the INS spectra of a similar order as that found in the C_{3v} molecular calculation. The further tilting modes are hardly visible in the INS spectra, in a region whereby signal is washed out through molecular recoil. The lower energy tetrahedral distortions, comprising Li-N bends also agree with our models, as does the A_1 molecular breathing mode.

Unlike the IXS, IINS is able to resolve librational features, and it is for these modes that greatest discrepancy between measurement and molecular modelling occurs. There is a strong and sharp feature in the INS at 19.8 meV, indicative of a librational feature. Examining the eigenvectors in the corresponding solid DFT confirms this to be the case, with this feature being attributed to the libration of the N1 NH_3 units. The remaining librations occur at lower energy, in a region of the INS between 14-17 meV of lower intensity. This broad features peaks at 16.1 meV and shows a number of unresolved features below this energy. This is indicative of a coupling to other internal modes in the solid, due to a lowering of site symmetry, principally the tetrahedral bend.

The lowest energy features in the INS are the external-modes in the crystal, the rigid-molecule translations and librations of the $Li(NH_3)_4$ units. These broad features are found between 1-8 meV, but interestingly there is an additional sharp feature in the INS at 2.7 meV. The sharpness suggests an internal mode demonstrating little dispersion, this internal nature also concurrent to the fact that this feature persists in all of the phases measured (including the highest temperature measurement). This is very close to the energy of NH_3 libration calculated in the 'ideal' T_d molecule, whereby N-H bonds are staggered with respect to Li-N bonds, and thus we may tentatively assign it as such and not a libration of the whole $Li(NH_3)_4$ molecule. That no such feature is witnessed in the solid or C_{3v} molecular calculations could be suggestive of a disorder about the Li-NH_3 in the protonated solid, absent in the deuterated crystal structures.

As ever with this fascinating compound we must ask ourselves, 'what kind of metal is this, that melts at such a low temperature'? Intermolecular interactions in the solid phases of $Li(NH_3)_4$ are dominated by H$\cdots$H contacts, as suggested by the strong isotope effect of there existing a plastic phase for $Li(NH_3)_4$ and not $Li(ND_3)$. We have demonstrated that there are no discernible difference in the internal dynamics of the $Li(NH_3)_4$ molecules through the solid phases of $Li(NH_3)$, and have revealed some interesting, low energy librational features that we believe warrant further examination. This would be particularly true for spectroscopic techniques that can examine this system through the solid-liquid transition.

AGS, KRR and PPE would like to thank the EPSRC for funding (grant EP/K002561/1). Keith Refson is thanked for advise on calculation, and the STFC are thanked for granting beamtime at the ISIS Spallation Neutron Source and for access to the SCARF supercomputing cluster. EZ acknowledges the NSF (DMR-1005413) for financial support and the Center for Computational Research at SUNY Buffalo for computational support.

References

1 E. Zurek, P. P. Edwards and R. Hoffmann, *Angew. Int. Ed.*, 2009, **48**, 8198–8232.

∗ Data from Said et al [7], as collected in Pinsook et al [8]

2 E. Zurek, X. D. Wen and R. Hoffmann, *J. Am. Chem. Soc.*, 2011, **133**, 3535–3547.
3 R. M. Ibberson, A. J. Fowkes, M. J. Rosseinsky, W. I. F. David and P. P. Edwards, *Angew. Chem. Int. Ed.*, 2009, **48**, 1435–1438.
4 A. M. Stacy and M. J. Sienko, *Inorg. Chem.*, 1982, **21**, 2294–2297.
5 V. L. Coulter, J. K. Gibson and N. Mammano, *J. Phys. Chem.*, 1984, **88**, 3896–3900.
6 H. Thompson, N. T. Skipper, J. C. Wasse, W. S. Howells, M. Hamilton and F. Fernandez-Alonso, *J. Chem. Phys.*, 2006, **124**, 024501.
7 A. H. Said, C. A. Burns, E. E. Alp, H. Sinn and A. Alatas, *Phys. Rev. B*, 2003, **68**, 104302.
8 U. Pinsook, R. Scheicher, R. Ahuja and S. Hannongbua, *J. Phys. Chem. A*, 2008, **112**, 5323–5326.
9 L. Varriale, N. Tonde, N. Bhalla and A. Ellis, *J. Chem. Phys.*, 2010, **132**, 161101.
10 P. C. H. Mitchell, S. F. Parker, A. L. Ramirez-Cuesta and J. Tomkinson, *World Scientific*, 2005, **Vibrational spectroscopy with neutrons**,.
11 S. Lovesey, *Oxford Scientific Publications*, 1984, **Theory of Neutron Scattering from Condensed Matter, Volume 1**,.
12 C. Andreani, D. Colognesi, J. Mayers, G. F. Reiter and R. Senesi, *Adv. Phys.*, 2005, **54**, 377–469.
13 J. Mayers and T. Abdul-Redah, *J. Phys. Condens. Matter*, 2004, **16**, 4811–4832.
14 J. Mayers, *User guide to VESUVIO data analysis programs for powders and liquids.*, 2011, **RAL Technical Reports**, RAL:TR–2001–003.
15 K. Maeda, M. Lodge, J. Harmer, J. Freed and P. Edwards, *J. Am. Chem. Soc.*, 2012, **134**, 9209–9218.
16 D. Colognesi, M. Celli, F. Ciloco, R. J. Newport, S. F. Parker, V. Rossi-Albertini, F. Sacchetti and J. Tomkinson, *Appl. Phys. A*, 2002, **74**, S64–S66.
17 J. Mayers and G. Reiter, *Meas. Sci. Technol.*, 2012, **23**, 045902.
18 S. J. Clark, M. D. Segall, C. J. Pickard, P. J. Hasnip, M. J. Probert, K. Refson and M. C. Payne, *Z. Kristallogr.*, 2005, **220**, 567–570.
19 J. Perdew, K. Burke and M. Ernzerhof, *Acd. Sym. Ser.*, 1996, **629**, 453–462.
20 A. J. Ramirez-Cuesta, *Comput. Phys. Commun.*, 2004, **157**, 226–238.
21 G. te Velde, F. M. Bickelhaupt, E. J. Baerends, C. Fonseca Guerra, S. J. A. van Gisbergen, J. G. Snijders and T. Ziegler, *J. Comput. Chem.*, 2001, **22**, 931–967.
22 E. J. Baerends, J. Autschbach, A. Bérces, F. M. Bickelhaupt, C. Bo, P. M. Boerrigter, L. Cavallo, D. P. Chong, L. Deng, R. M. Dickson and et al., ADF2010.01, http://www.scm.com.
23 B. Hammer, L. B. Hansen and J. K. Norskov, *Phys. Rev. B,*, 1999, **59**, 7413–7421.
24 S. H. Vosko, L. Wilk and M. Nusair, *Can. J. Phys.*, 1980, **58**, 1200–1211.

1 Further Information

Samples of $Li(NH_3)_4$ were prepared using the same approach as documented previously.[15] Anhydrous and de-gassed NH_3 was condensed in stoichiometric amounts onto a clean sample of Li metal, within a specially designed flat sample cell that was pre-cleaned and heat treated. The golden liquid was then frozen to the bronze coloured solid and sealed under vacuum, henceforth maintained at cryogenic temperatures at all times to avoid any decomposition. IINS and DINS measurements were performed on the high-resolution TOSCA[16] and VESUVIO[17] instruments at the ISIS spallation neutron source, Chilton, UK. In order to assign the features present in the IINS spectra, computational modelling of the $Li(NH_3)_4$ system was performed at the level of fully-periodic density functional theory using the plane-wave (PW) CASTEP code.[18] The unit cell for the system was constructed from the crystal structures as detailed in reference [2]. This unit cell comprises 16 $Li(NH_3)_4$ units, and all calculations were thus performed on this 272 ion system. A PW cutoff of 650 eV was specified for each calculation, with k-point sampling performed on a $2\times2\times2$ Monkhorst-Packhouse grid. The exchange correlation functional of Perdew, Burke and Erzerhoff (PBE)[19] was chosen and normconserving pseudopotentials were used to describe atomic core potentials.

The internal geometry of ions within the system were allowed to optimise within a fixed cubic cell of identical primitive lattice parameter to that determined by neutron diffraction, $a = b = c = 14.78342$ Å . Optimisations were undertaken with symmetry specified and maintained as $I\bar{4}3d$ (Phase II), to avoid any possible antiferromagnetic behaviour suggested in phase III. Energy and forces were converged to better than $1e^{-}9$ eV and $1e^{-2}$ eVÅ^{-1} respectively. Phonon frequencies and eigenvectors were determined using linear response density functional theory as implemented within CASTEP.

The IINS spectra have then been modelled using the aCLIMAX code[20] as is now standard practise for IINS analysis.

The molecular geometry optimizations and frequency calculations were carried out with the Amsterdam Density Functional (ADF) package[21,22]. We have applied the revised Perdew, Burke and Ernzerhof (revPBE) non-hybrid gradient density functional[19,23] and the Vosko-Wilk-Nusair (VWN) local spin density approximation[24], along with an all-electron even-tempered valence quadruple-zeta basis set with three polarization functions and one set of diffuse s, p, d and f Slater Type Orbitals (ET-QZ3P(1)) for Li and H and a triple-zeta Slater type basis with polarization functions (TZP) and a 1s frozen core for N from the ADF basis set library. These computational settings have previously been employed to study various species that may be pressent in metal-ammonia solutions[1]

The essentially unchanged dynamics of the system in each phase is also demonstrated in the DINS measurements. Figure 1 presents the fitted neutron Compton profiles, equations 2 and 3, in $Li(NH_3)_4$, as determined from DINS measurements. No differences were found between measurements on the different solid phases of the metal, and so only data collected at 4 K are presented here.

Deviations from an isotropic harmonic approximation in $J(y)$ for the proton can be accounted for by an expansion of a gaussian term to include higher order Hermite polynomials. We find that data fits well including up to H_4,

$$J_H(y) = 2\pi\int_{|y|}^{\infty} pn(p)dp = \frac{1}{\sqrt{2\pi\sigma_H^2}}\exp\left(\frac{-y_H^2}{2\sigma_H^2}\right)(1+\frac{c_4}{32}H_4). \qquad (3)$$

The determination of the width of the momentum distribution, σ_H, allows for the direct measurement of the average kinetic energy of the proton through the relation $\langle E_K\rangle = 3\hbar^2\sigma_H^2/2M$.

It can be seen from figure 1 that there is only negligible difference, within the error of the fit, of the Compton profiles for $Li(NH_3)_4$ in the solid phases. We also saw no change in measurements at 100 K. This reflects the truly molecular nature of this metal, with the proton momentum distribution being dominated by contribution from the N-H bond.